DESIGN AND ANALYSIS OF A HYBRID FEED ANTENNA FOR A FLUX-FLOW OSCILLATOR INTEGRATED 460 GHz SIS RECEIVER

M.-H. Chung and M. Salez
DEMIRM, Observatoire de Paris, 61, avenue de l'Observatoire, 75014 Paris, France
E-mail : moon-hee.chung@obspm.fr

Abstract

We have designed a 460 GHz FFO-driven integrated SIS receiver in which the signal is fed via a quasi-optical hybrid antenna feeding system. Since in such quasi-optical SIS receivers the contribution of the quasi-optics to the overall receiver noise is considerable, it is important to be able to analyze the antenna efficiency in order to optimize its coupling and improve the noise temperature of the receiver. The goal of this paper is an attempt to analyze the gaussian coupling efficiency, far-field pattern and loss of the system, applying the geometrical optics-physical optics combined method to our hybrid integrated feed antenna. The computation of the loss contributed by different quasi-optical solutions can be a decision factor for selecting one particular design (optics materials, geometries, and configuration). Quite commonly adopted solutions employ a substrate hemispherical lens in conjunction with (or without) an objective lens of HDPE or Teflon located in the Fresnel region of the hemispherical lens. Such solutions have advantages and drawbacks, and other solutions, better for the receiver noise, may exist. In addition, computing the radiation characteristics of the quasi-optical system will be useful to interpret the integrated receiver measured performances and evaluate the diverse noise sources in this complicated system. A numerical tool based on the the ray-tracing and diffraction mixed approach was implemented to examine the radiation characteristics of the feed structure of FFO integrated SIS receiver.

1 Introduction

Flux-Flow Oscillators (FFO) integrated with SIS receivers have been proposed as an attractive alternative to commonly used submillimeter wavelength local oscillators; they are compact, low-mass and low-power consumption devices, and they can provide individually optimized LO power to the SIS mixers of a focal plane heterodyne receiver array. The most recent and extensive experimental work aiming at producing a fully operational-and phase-locked-integrated SIS receiver, for array applications, has been done by Shitov *et al* [1].

There is a growing need for heterodyne focal plane imaging arrays, either to speed up commonly time-consuming mapping observations, or to do interferometry with a single-dish telescope. In this context we have designed an integrated FFO SIS receiver chip for 460 GHz, and the receiver is now under construction. Our goal is to test the mixing performance of this new kind of superconducting submillimeter receivers, using slightly different technological choices than those of [1], for a frequency range of typical interest for radioastronomical studies.

Since the relatively complicated superconducting circuits (FFO, integrateddiplexer) require more contact pads which hardly fit within the regular dielectric chips for waveguide mounts, the quasi-optical solution is generally the adopted one to feed the FFO integrated SIS mixers. It usually consists of a combination of planar antenna and dielectric lens, and for array applications, either the 'fly's eye' configuration-where each planar antenna and integrated receiver pixel has its own dielectric lens-and the 'single-lens' configuration-where only one lens illuminates the whole array can be considered. Several other options can be considered for the design, depending on the type of planar antenna (bow-tie, double-dipole, double-slot, log-periodic, etc), the type of lens (elliptic, hyperhemispherical, extended hemispherical), the lens material and the nature of the substrate on which the superconducting receiver is fabricated.

Choosing among these design options not only drives the receiver optical coupling scheme and geometry, but it may also have consequences on the RF losses which often considerably contribute to the total noise of receiver-although the sensitivity of the SIS mixer itself is quantum noise limited [2]. Therefore, it is necessary to analyze in detail the RF characteristics of the quasi-optical solutions considered to estimate their impact on the receiver system.

Most of all, the radiation properties of the FFO integrated SIS mixer is critical in the case of a focal plane imaging array receiver in which the beam pattern of the feed antenna must be well matched to the radiotelescope optics. In particular, it is important to pay attention to the feed antenna's directivity and sidelobes. For an array, high directivity with low sidelobes is required, to optimize the pixels aperture efficiency and to have each pixel sample the sky in a clean way.

The hybrid feed antenna for our quasi-optical receiver consists of an extended hemispherical lens with a double dipole as the elementary radiator and, potentially, one additional-'objective'-dielectric lens. This type of integrated lens antenna has been widely used in the millimeter and submillimeter wavelength domain [4]. Yet our goal was to determine, before finalizing the receiver's design, whether this configuration was the best suited for our purpose, given our experimental constraints.

A numerical tool was implemented to estimate the radiation properties (gaussian coupling, directivity, sidelobes) of our quasi-optical feed system and to investigate the influence on those of the lenses geometry, such as the hemispherical lens extension. Since a direct application of the diffraction theory for our hybrid feed antenna would be very time consuming, we used a mixed approach[7], combining a ray-tracing technique within the substrate lens and the diffraction theory to calculate the far fields.

2 Design aspects

Hybrid antennas-substrate lenses combined with elementary planar antennas-are widely used in open structure integrated receivers. One reason is that they solve the problem of substrate modes at submillimeter wavelengths-the dielectric lens can be considered as half space. Most of the radiation occurs within the substrate, yet some amount still radiates in the air, resulting in extra RF losses. If a high dielectric constant material cannot be used for the lens-or is not wished-then a back plane reflector must be placed about l/4 wavelength away from the planar antenna to fold the back-radiated beam onto the main beam in the lens, without modifying its radiation pattern. Most people use silicon lenses for this reason; the power loss in the air side of double-slot antennas on silicon($\epsilon = 11.7$) is only 8%[5]. However, silicon lenses induce important reflection losses at their front surface, which must be minimized by hard-to-manufacture antireflection coating.

Our choice of dielectric material for the lens was mostly driven by SIS technology-our superconducting FFO-SIS receiver is made on fused quartz substrates ($\epsilon = 3.8$). Having a different dielectric for the lens would cause spurious and inevitable reflections at the interface, and restore potential substrate modes in the receiver chip. Fused quartz is not a bad choice, compared to silicon, for spillover and polarization efficiencies. And the lower dielectric constant of fused quartz compared to silicon gives an advantage of lower reflection loss without anti-reflection layer. However, due to its low dielectric constant, the power loss radiated into the air side in our case is about $20 \sim 30\%$, and therefore a metallic back reflector must be used. This can be done because we use microstrip structures and double-dipole antennas, hence leaving most of the chip's surface unoccupied. The beam pattern of the double-dipole antenna does not change with the reflector. The double-dipole size and spacing were determined so as to produce a symmetric radiation pattern in the E- and H-plane[3].

If we place the elementary radiator at the aplanatic point of the hemispherical lens (i.e. R/n, where R is the lens radius and $n = \sqrt{\epsilon_r}$, as one often conveniently does, it is then necessary to add an objective lens to enhance the directivity of the overall feed system. But there is a possibility of using a simpler configuration, with no objective lens. This depends on the elementary radiator's position relative to the center of the hemispherical lens-the hemispherical lens extension. Büttgenbach [10] defined the hybrid antenna as a special case of extended hemispherical lens with the extension length beyond the aplanatic point, combined with a planar feed antenna. Then the lens, which approximates an elliptical lens, is diffraction-limited. He proposed to use this hybrid antenna as an alternative to the hyperhemispherical lens antennas used in conjunction with an objective lens, and discussed related problems of gaussian coupling efficiency. These feed structures seem very attractive because they allow simpler designs and low cost fabrication. As a consequence, we have considered with no a priori the addition of an objective lens and the extension length of the hemispherical lens as a free parameter for our feed design.

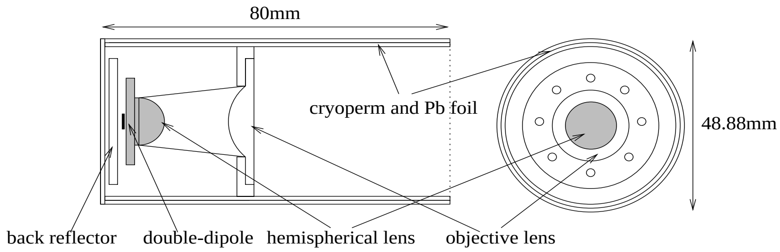

Figure 1: Feed structure of a FFO integrated SIS receiver

When the extended hemispherical lens is diffraction-limited and use without objective lens, its radius determines the f-number of the quasi-optical system. Therefore several geometrical factors had to be taken into account as boundary conditions.

The FFO being a very sensitive device to magnetic field, one must enclose FFO-integrated SIS receivers in magnetic shielding assemblies. In our case, the shield consists of a cylinder with one closed end, made of two concentric 1.47-mm thick Cryoperm layers and one inner 0.25-mm thick lead foil layer, in order to provide approximately 70 dB of magnetic shielding at 4.2K[6]. To maximize the shielding and reduce the open end effect, the length-to-diameter ratio should be as large as possible. The length of our cylinder assembly is 80mm and its inner diameter is 42.5mm. So, we have to make a very compact quasi-optical mixer design, with a f-number larger than 8.

Figure 1 shows the overall feed structure of our FFO integrated SIS mixer.

3 Theoretical analysis

3.1 Hemispherical lens fed by double-dipole antenna

Figure 2 shows the structure to be analyzed. To calculate the radiation properties of the hemispherical lens antenna, the ray tracing and diffraction theory similar to the approach of [7] is used in this report. We consider here only on-axis feed position case but this method can be easily generalized to off-axis feed positions. Ray-tracing can be used to treat the radiation in the lens only because its dimensions are much larger than the wavelength.

The double-dipole antenna is located on the planar surface of the hemispherical lens with distance, e from the center of hemispherical lens. The electromagnetic fields on the internal curved surface of the lens, (θ_s, ϕ_s) coordinate system, can be determined from the far-fields of the double-dipole antenna, $\overrightarrow{F}(\theta_d, \phi_d)$, assuming that the size of lens is enough large compared to the wavelength to satisfy the conditions of the geometrical optics,

$$\overrightarrow{E_s}(\theta_s, \phi_s) \quad = \quad \frac{jk_d e^{-jk_d r_d}}{4\pi r_d} \left[F_{\theta_d}\left(\theta_d, \phi_d\right) \widehat{\theta_d} + F_{\phi_d}\left(\theta_d, \phi_d\right) \widehat{\phi_d} \right] \tag{1}$$

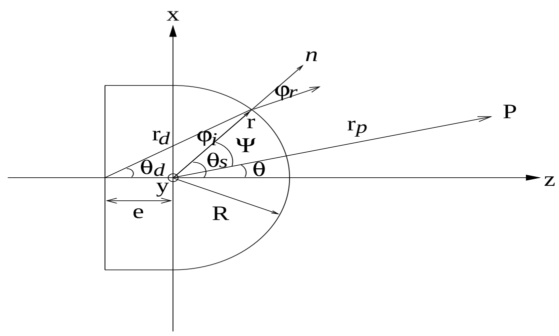

Figure 2: Coordinate system for the analysis of hemispherical lens

$$\overrightarrow{H_s}(\theta_s, \phi_s) = \frac{1}{\eta_d}\left(\hat{n} \times \overrightarrow{E_d}\right) \tag{2}$$

where k_d, η_d are the propagation constant and intrinsic impedance in the substrate lens respectively. The transmitted fields on the external curved surface of lens are found using the Fresnel transmission coefficients,

$$E'_{\theta_s} = T_{||} E_{\theta_s} \cos(\varphi_r) \tag{3}$$

$$E'_{\phi_s} = T_{\perp} E_{\phi_s} \cos(\varphi_r) \tag{4}$$

The parallel and perpendicular Fresnel coefficients are,

$$T_{||} = \frac{2n\cos\varphi_i}{n\sqrt{1 - n^2\sin^2\varphi_i} + \cos\varphi_i} \tag{5}$$

$$T_{\perp} = \frac{2n\cos\varphi_i}{n\cos\varphi_i + \sqrt{1 - n^2\sin^2\varphi_i}} \tag{6}$$

where $\varphi_i = \theta_s - \theta_d$

The equivalent surface electric and magnetic current on the external curved surface of the lens are,

$$\overrightarrow{J_s} = \hat{n} \times \overrightarrow{H'_s} \tag{7}$$

$$\overrightarrow{M_s} = -\hat{n} \times \overrightarrow{E'_s} \tag{8}$$

The far-fields at the observation point P from the hemispherical lens can be calculated using diffraction theory,

$$E_\theta = -\frac{jke^{-jkr_p}}{4\pi r_p}(L_\phi + \eta N_\theta) \tag{9}$$

$$E_\phi = \frac{jke^{-jkr_p}}{4\pi r_p}(L_\theta - \eta N_\phi) \tag{10}$$

where the radiation vectors $\overrightarrow{N}$ and $\overrightarrow{L}$ are defined as the followings,

$$\overrightarrow{N}(\theta,\phi) = \int\int_S \overrightarrow{J_s}(\overrightarrow{r})e^{jkR\cos\Psi}ds \quad (11)$$

$$\overrightarrow{L}(\theta,\phi) = \int\int_S \overrightarrow{M_s}(\overrightarrow{r})e^{jkR\cos\Psi}ds \quad (12)$$

k is the propagation constant in the free space, R is the radius of the hemispherical lens, Ψ is the angle between the integration point and the observation point, and the integration is done on the surface S of the hemispherical lens.

3.2 Hyperhemispherical lens combined with an objective lens

By definition, a hyperhemispherical lens is an extended hemispherical lens with the elementary radiator located at the aplanatic point. Such a feed system is characterized by a high gaussian coupling efficiency. However, the directivity is not sufficient to match most f-numbers of practical use in receiver applications, and it must therefore be used together with an objective lens to increase the global directivity.

Even though one needs a full-wave numerical modeling to analyze the radiation properties in the Fresnel zone which is located between the hemispherical lens and the objective lens, we believe that the ray-tracing method can provide a first approximation of the radiation pattern of the extended hemispherical lens combined with an objective lens[8]. In the calculations, we assume that the objective lens has hyperbolic surface on the back side and a plane surface on the front side as shown in Fig.3. To simplify the ray-tracing method, the curved surface of the hemispherical lens is assumed to have an anti-reflection layer - to neglect the reflected rays.

Since we assume the hyperhemispherical lens to be ideal, we can virtually move the focal point, $-R/n$, of the hyperhemispherical lens into the one, $-nR$, of the objective lens. In the Fig.3, n, R, D, F are respectively the refractive index and radius of the hyperhemispherical lens, and the diameter and focal length of the objective lens. In the diffraction limit, the diameter D will define the feed system's FWHP (Full Width Half-Power) .

4 Results of computation and design considerations

To confirm the validity of our computer program, we compared the calculated results with the published ones of [7] for the same data and found good agreements.

The radiation properties of the feed structure of FFO integrated SIS receiver were then calculated, first with an extended hemispherical lens, the extension length of which could be varied, and no objective lens.

Figure 4 shows the beam pattern of our double-dipole antenna, used as an elementary radiator on the planar surface of the fused quartz hemispherical lens. The length

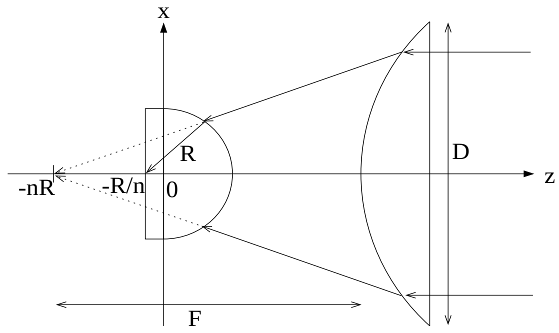

Figure 3: Hyperhemispherical lens combined with an objective lens

of the double-dipole antenna is $0.5\lambda_d$, its distance, $0.4\lambda_d$ and the distance of the back reflector, $0.25\lambda_d$ where λ_d is the wavelength of 460 GHz in the fused quartz($\epsilon = 3.8$).

Figure 5,6,7,8, and 9 show the far-field pattern at 460 GHz of the hemispherical lens, the diameter of which is 12 mm, for different extension lengths varied from 2.5 to 6.5mm by steps of 1.0mm. The extension length of 3mm approximately corresponds to our R/n. We note a good E and H plane symmetry in Fig.10. As with the elliptic lens, the phase, shown in Fig.10, is flat (top-hat) across the main lobe. The extension length referred here is in fact the distance from the center of hemispherical lens to the back reflector. As expected, the radiation lobe of the hemispherical lens becomes sharper when the extension length increases; the sidelobes level decreases; it seems to converge toward a diffraction limit.

Figure 11 shows the directivity and gaussian coupling efficiency of the hemispherical lens with the variation of the extension length. The gaussian coupling efficiency is defined in (13)[9],

$$\eta = \frac{\left| \int \int_S \overrightarrow{E_g} \cdot \overrightarrow{E_a} \, ds \right|^2}{\int \int_S \left| \overrightarrow{E_g} \right|^2 ds \int \int_S \left| \overrightarrow{E_a} \right|^2 ds} \tag{13}$$

where $\overrightarrow{E_g}$ is the electric field represented by the incident gaussian beam, $\overrightarrow{E_a}$ is the field of the hemispherical lens antenna and S is the spherical surface of integration centered on the position of the hemispherical lens antenna. The amplitude and phase of electric field of the incident gaussian beam, $\overrightarrow{E_g}$, must be varied to find the maximum gaussian coupling efficiency. As already mentioned in [7], Figure 11 shows that when the extension length increases, the gaussian coupling efficiency decreases while the directivity of the hemispherical lens increases to reach a maximum value around the extension length of 5.5 mm. Past the extension length of 5.5 mm, the side lobe levels increase again, hence degrading the directivity of the extended hemispherical lens.

Now, we made similar calculations in the case of a hyperhemispherical lens combined with an objective lens. For practical reasons (the magnetic shield) our objective lens has a diameter of 18 mm, a focal length of 41.78 mm. It is made of Teflon

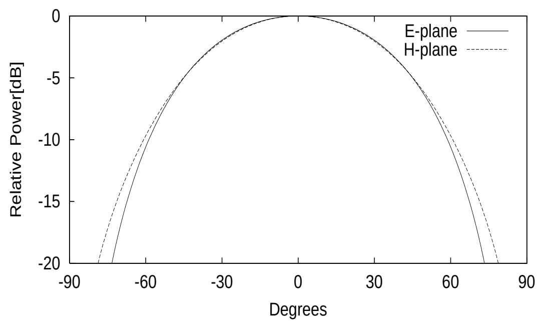

Figure 4: Beam pattern of double-dipole antenna with back reflector

($\epsilon_r = 2.3$)-a common choice at these frequencies-and is 4.0 mm thick at the widest. Again to simplify the ray-tracing technique, we assumed that its front side is coated with an anti-reflection layer.

Figure 12 shows the calculated beam pattern of hyperhemispherical lens combined with an objective lens at 460 GHz. The calculated directivity is 34.9 dB and the estimated FWHP is $2.7°$. This is close to the FWHP of about $2.49°$at 460 GHz expected from diffraction theory for our objective lens, according to (14):

$$\theta_{FWHP} \simeq 1.2\frac{\lambda}{D} \tag{14}$$

It means that the hyperhemispherical lens combined with the objective lens reaches the diffraction limit.

From the calculated results, it would seem a priori a reasonable choice to select the maximum gaussian coupling efficiency solution, that is, a hyperhemispherical lens with an objective lens which increases the directivity of the system, and makes it diffraction-limited. But the calculated result of the gaussian coupling efficiency is always an optimized value: it needs the appropriate gaussian beam to obtain this maximum coupling efficiency. Experimentally, it is very difficult to obtain, so as to measure the gaussian coupling efficiency[7],[10]. Also, the coupling efficiency depends on other factors, such as antireflection coating, alignment, etc. Figure 13 shows the calculated gaussian coupling efficiency with variations of the amplitude and phase of the incident gaussian beam. We see that the coupling efficiency is very easily affected by the amplitude and phase of the incident beam. This means that only a small misalignment or error in focusing will get us off the maximum gaussian coupling efficiency.

On the other hand, we have calculated the gaussian coupling efficiency and directivity of a hemispheric lens without objective lens, and have shown that for an extension length past beyond the aplanatic point, the directivity reaches a maximum, and the beam is diffraction-limited. We believe this criterion is more important than optimum coupling efficiency in practice, especially from the point of view of making reliable and optimized feed arrays for spectro-imaging systems. By choosing the lens diam-

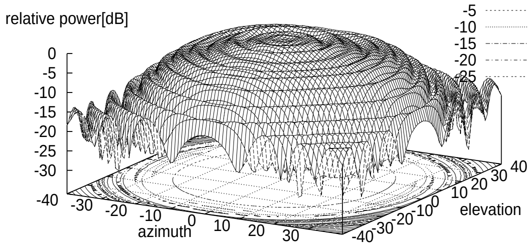

Figure 5: Beam pattern of hemispherical lens for the extension length of 2.5 mm

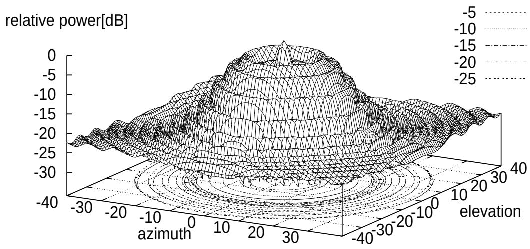

Figure 6: Beam pattern of hemispherical lens for the extension length of 3.5 mm

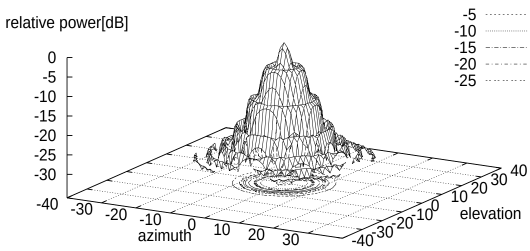

Figure 7: Beam pattern of hemispherical lens for the extension length of 4.5 mm

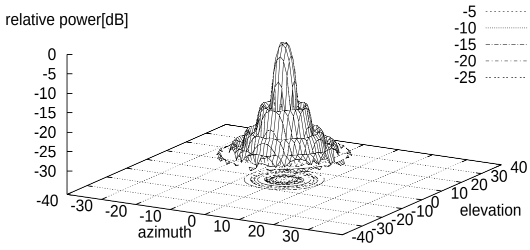

Figure 8: Beam pattern of hemispherical lens for the extension length of 5.5 mm

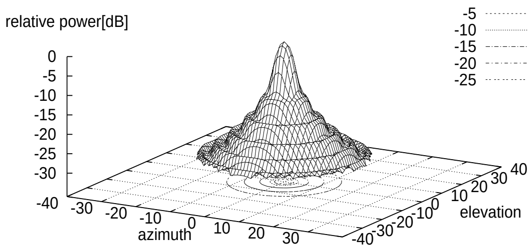

Figure 9: Beam pattern of hemispherical lens for the extension length of 6.5 mm

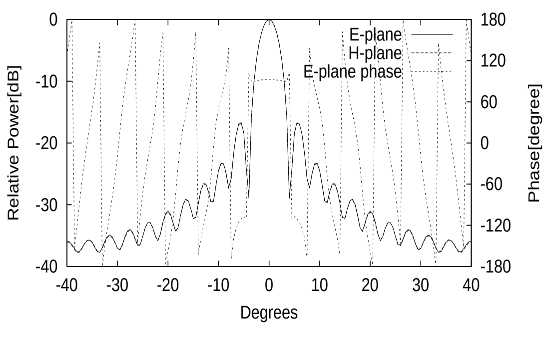

Figure 10: E and H-plane power pattern and phase for the extension length of 5.5mm

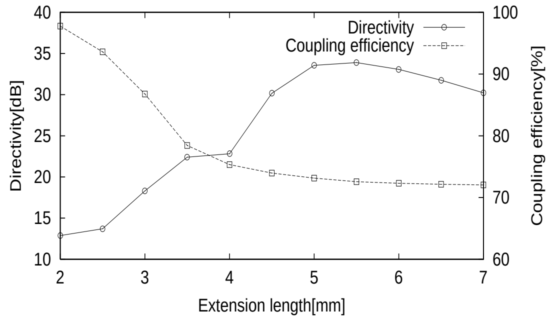

Figure 11: Directivity and gaussian coupling efficiency of the hemispherical lens at 460 GHz

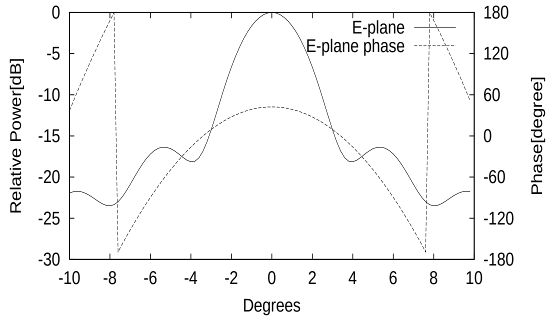

Figure 12: Far-field pattern of hyperhemispherical lens combined with an objective lens at 460 GHz

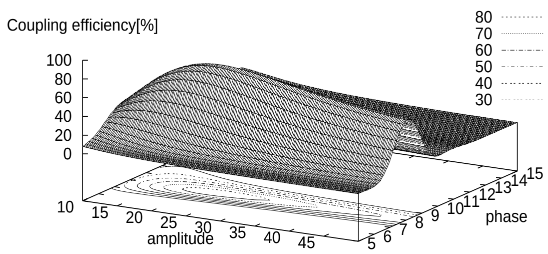

Figure 13: Calculated gaussian coupling efficiency of the hemispherical lens fed by double-dipole antenna at 460 GHz for the extension length of 3mm and the amplitude and the phase are for the electric field representation of the incident gaussian beam.

eter (hence the beam f-number) and dielectric material (hence minimizing the risk of reflection loss and back-radiated power loss), we can not only design an efficient lens for a pixel, but make it easy to fabricate and low-cost. It remains to decide whether the best configuration for an array receiver using these extended hemispherical lenses is the fly's eye or one single lens illuminating many pixels. Probably the former is the best, when we want performance uniformity among the pixels-our drive to make FFOs initially. Our future work will include calculations of antenna gain and directivity for different off-axis positions of the double-dipole antennas within the lens plane.

Another advantage of this solution without objective lens concerns the associated RF loss and its influence on the SIS receiver noise. Aside from reflection losses, the objective lens has dielectric losses which will contribute to the RF noise, especially since large Teflon lenses may not cool down uniformly, while fused quartz lenses on the mixer block are certain to be at 4.2 K (be it the SIS device temperature) .

5 Conclusion

We implemented a numerical tool based on the the ray-tracing and diffraction mixed approach which is similar to [7] to examine the radiation characteristics of the feed structure of our FFO integrated SIS receiver, which consists of an extended hemispherical lens fed by a double-dipole antenna, backed by a plane reflector, and with or without an objective lens. In the latter case (no objective lens), we found results very similar to those of [7], and confirming the experimental results of [10], showing a maximum of the directivity obtained for a lens extension larger than R/n -the hyperhemispherical lens plane of truncation. Then, the beam's FWHP almost reaches the diffraction limit. In our case, this extension length is about $0.9R$, and the beam divergence is small enough to be compatible with our FFO receiver design, where the mixer must be housed in the rear end of a rather long cylindrical magnetic shield. We believe it is not necessary to use an objective lens, even though the calculated gaussian coupling efficiency of this hybrid lens antenna is smaller than in the case of a hyperhemispherical lens: what seems most important to us when selecting the configuration of the feed system-especially in view of an array application-is the beam quality and directivity. Furthermore, the gaussian coupling efficiency is very hard to measure at submillimeter wavelengths since it requires the measurement of absolute powers[10]. There is no clear experimental indication, therefore, that this parameter is so drastically reduced with our design that it should forbid it. In addition, there is one secondary-but not negligible for an array-advantage in using extended hemispherical lenses without objective lens: the low fabrication cost compared to expensive elliptic lenses.

References

[1] S.V.Shitov, V.P. Koshelets, A.M.Baryshev, L.V. Filippenko, Th.de Graauw, J.R. Gao, W.Luinge, H. van de Stadt, N.D.Whyborn, P.Lehikoinen, "Development of superconducting integrated receiver for application in imaging arrays," *Proc. 7th Intl. Conf. Space Terahertz Technology*, 1996.

[2] Tucker J.R. and Feldman M.J., "Quantum detection at millimeter wavelengths," *Rev. Mod. Phys*., vol. 57, pp. 1055-1113, 1985.

[3] A.Skalare, "SIS Heterodyne receivers using broadside and endfire double dipole antennas," Internal Report, S.R.O.N., Postbox 800, 9700 AV Groningen, the Netherlands, February, 1993.

[4] M.C.Gaidis, H.G.LeDuc, M.Bin, D.Miller, J.A.Stern, and J.Zmuidzinas, "Characterization of low-noise quasi-optical SIS mixers for the submillimeter band," *IEEE Microwave Theory Tech.,*vol.44,no.7, pp. 1130-1138, 1996.

[5] M.Kominami, D.M. Pozar, and D.H. Schaubert, "Dipole and slot elements and arrays on semi-infinite substrates," *IEEE Trans. Antennas Propagat*. vol.33, pp.600-607, June 1985

[6] Private communication with Larry Maltin of Amuneal Manufacturing Corp.4737 Darrah Street Philadelphia, PA 19124-2705

[7] D.F.Filipovic, and G.M.Rebeiz, "Double-slot antennas on extended hemispherical and elliptical quartz dielectric lenses," *Intl. J. Infrared Millimeter-Waves*, vol.14, No.10, pp 1905-1924, 1993.

[8] M.J.M.Van der Vorst, P.J.I. de Maagt, and M.H.A.J. Herben, "Electromagnetic modeling of objective lenses in combination with integrated lens antennas," *Proc. 9th Intl. Conf. Space Terahertz Technology*, pp.389-395, 1998.

[9] S.E.Schwarz, "Efficiency of quasi-optical couplers," *Intl. J. Infrared Millimeter-Waves*, vol.5, No.12, pp 1518-1525, 1984.

[10] T.Büttgenbach, "An improved solution for integrated array optics in quasi-optics mm and submm receivers: the hydrid antenna," *IEEE Microwave Theory Tech.,*vol.41,no.10, pp. 1750-1761, 1993.